

AN INTEGRATED APPROACH TO THE STRUCTURAL ASSESSMENT OF HISTORIC BUILDINGS: the case of St. Angelo Church in Anagni

Ricardo Maia Avelino
ETH Zürich, Switzerland, maia@arch.ethz.ch

Carlo Oliveri
University of Salerno, Italy, colivieri@unisa.it

Elodie Donval
CSTB/École des Ponts, France, elodie.donval@cstb.fr

Rebecca Fugger
Roma Tre University, Italy, rebecca.fugger@uniroma3.it

Matteo Lai
Università degli Studi di Cagliari, Italy, matteolai@unica.it

Mariaceleste Lasorella
Politecnico di Bari, Italy, mariaceleste.lasorella@poliba.it

Ylenia Saretta
University of Padova, Italy, ylenia.saretta@phd.unipd.it

Anjo Weichbrodt
ETH Zürich, Switzerland, aweichbrodt@ethz.ch

Marialuigia Sangirardi (corresponding author)
University of Oxford, United Kingdom, marialuigia.sangirardi@eng.ox.ac.uk

ABSTRACT

This paper tackles the problem of the safety assessment of St. Angelo church in Anagni (Italy) through an integrated approach linking geometrical survey with structural analysis. A historic analysis is first performed collecting information from ancient drawings and on-site observations identifying the main construction phases and interventions executed throughout the centuries and highlighting the different materials adopted in the construction. Terrestrial and aerial close-range photogrammetry is executed to reconstruct the geometry of both the interior and the exterior of the building, resulting in

Cover picture:
Vault in the central nave of Sant'Angelo church.

a fully three-dimensional digital model of the building and its surroundings. From this model, the main structural elements of the structure were identified, and a structural assessment was performed adopting the lower-bound theorem of limit analysis. The main vaults are analysed through a graphics slicing technique and the overall geometric safety factor of the representative structural section of the church is obtained. The paper illustrates a pipeline adapted to the assessment of existing structures, where safety factors can be obtained in a relatively short time directly from the data obtained through the survey and with fair compromise between complexity and accuracy. Coherent and appropriate use of modern technologies for geometrical survey and simple and clear mechanical theories allowed a multidisciplinary group of architects, conservators, and structural engineers to carry out a preliminary structural assessment of St. Angelo Church under gravitational loads. The conclusions drawn in light of the results of this analysis is that the Church can be considered safe.

SOMMARIO

UN APPROCCIO INTEGRATO PER LA VALUTAZIONE DELLA SICUREZZA STRUTTURALE DEGLI EDIFICI STORICI: il caso della Chiesa di Sant'Angelo ad Anagni

In questo articolo viene affrontato il problema della valutazione della sicurezza della chiesa di Sant'Angelo ad Anagni (FR), presentando la metodologia adottata. È stata dapprima eseguita un'analisi della storia dell'edificio, ricostruendo a partire dai disegni storici e dalle ispezioni in sito, la sequenza costruttiva e le diverse fasi che, susseguendosi, hanno determinato l'attuale configurazione della chiesa. Con l'ausilio di tecniche di fotogrammetria è stata ricostruita fedelmente la geometria sia dell'interno, che dell'esterno della Chiesa, rendendo possibile la creazione di un modello geometrico tridimensionale, sulla base del quale eseguire le analisi strutturali, secondo i principi dell'analisi limite e, in particolare, riferendosi al teorema statico (o del limite inferiore). Viene presentato dunque lo studio di dettaglio di una sezione trasversale, assunta di sufficiente generalità, a valle di un esempio di calcolo della spinta trasmessa dalla volta a crociera che sovrasta la navata centrale. Lo studio della sezione con i metodi tradizionali della statica grafica consente di valutare infine un fattore di sicurezza geometrico, considerato qui rappresentativo delle condizioni della struttura rispetto ai carichi gravitazionali, considerati nel calcolo. Con questo contributo si intende mostrare come l'uso efficiente, consapevole e combinato di strumenti avanzati di rilievo fotogrammetrico e di metodi di analisi relativamente semplici abbia consentito ad un gruppo costituito da ingegneri, architetti, conservatori, di valutare la sicurezza, da un punto di vista statico, della chiesa di Sant'Angelo.

KEYWORDS | PAROLE CHIAVE

Architectural Heritage, Safety Assessment, Masonry, Equilibrium, Limit analysis
Patrimonio architettonico, Verifiche di sicurezza, Muratura, Equilibrio, Analisi limite

INTRODUCTION

Preservation of historic masonry structures is an important concern for modern societies, needing to compromise between development, construction of new infrastructures and conservation of the built environment [1]. Structural analysis is required to assess the safety of these buildings, setup maintenance programs, design and target protection measures in case of possible damages triggered by natural or man-induced hazards. An effective methodology needs to rely on the cooperation of professionals, namely architects and engineers, often dealing with challenging and sophisticated tasks [2].

When working with monuments and historic buildings in general, one of the main difficulties in approaching their structural safety assessment is related to their unique and complex geometry [3]. Acquiring their geometry with high precision is a resource and time consumption task [4]. Moreover, determining the material properties used in the existing building is challenging, especially because in most of the cases this construction happened in multiple phases, using different materials and construction techniques which might have taken place during the years or, not rarely, centuries.

Assessing the safety of monuments in a general sense is directly related with the calculation of safety factors for the building in its current state and considering additional variable and exceptional loads, such as wind or earthquakes, that might lead the structure to collapse [5].

Currently, most of the available numerical structural analysis tools are developed to analyse steel or concrete structures, such as linear finite-element analysis (FEM), and do not particularly yield on the calculation of safety factors. Moreover, for the construction of reliable and realistic FEM models, determining the material properties is required and this is not always possible when dealing with historic buildings [6], essentially for invasiveness related issues. As a consequence, often monuments and historic buildings are approached with either inappropriate tools or with cumbersome models that do not always provide reliable results.

A revision in the approach to assess the structural behaviour of monuments is therefore needed, resulting in proper safety factors and building models that are well aligned with the typical input data that can be acquired through surveys.

The structural response of historic buildings is governed by geometry against both gravitational and exceptional actions such as earthquakes, or settlements [7,8]. Limit analysis can be applied as the theoretical background for combining geometry-intensive data and the required safety factors. Specifically, the lower-bound theory of limit analysis states that a structure is safe if an admissible stress state can be found, in equilibrium with the applied loads and respecting material properties in every point of the structure.

By adopting Heyman's assumptions [9,10] of no tensile strength, infinite compressive strength and no sliding, masonry structures can be framed within the Limit Analysis framework. As a result, admissible stress states in masonry are equivalent to compressive force paths contained within the geometry of the structure. These concepts link limit analysis to known structural assessment tools known since Hooke [11] and which have been applied to multiple historic monuments, such as

St. Peter's Church [12], and used in combination with slicing techniques [13,14,15]. Recent methods have extended this approach to 3D structures by searching compressive membranes contained within the geometry of the structure [16,17] or discrete compressive networks [18,19].

This paper presents the outcomes of the fieldwork performed during the 3rd edition of the Historic Masonry Summer School, held in Anagni (Frosinone, Italy). The 10 days course gathered international students with a diverse background in history, architecture and structural engineering, who took classes about structural assessment of masonry structures, geometry surveying of existing buildings and monuments, and historic survey. The skills acquired during the lectures were then applied by addressing the case study of three different monuments in the city of Anagni. This paper presents the assessment of St. 'Angelo Church which is executed through an integrated approach, linking the geometric survey executed with the structural analysis based on limit analysis tools which require as input exclusively the acquired geometry.

The paper is organised as follows: First, the methodology adopted throughout the survey and structural analysis is explained. Following, the case study is introduced and results obtained from the surveying expedition and geometric reconstruction are presented. Then, the results of the structural analysis are summarised with the computation of safety factors to the structure. Finally, the conclusion is presented highlighting the significance of this experience and pointing to further work.

METHODOLOGY

This section discusses the methodology adopted for the assessment of St. Angelo Church. We list the technical aspects characterising the survey phase, including physical history research, preliminary measurement survey, close-range photogrammetry and structural analysis.

Physical history research

The research on materials and construction phases was performed reviewing the limited available publications and interviewing church staff and neighbours of the St. Angelo Church and will be detailed in the following. The information was then integrated with in situ observations, focusing on construction and intervention sequences and on the techniques and materials employed. Some parts of the buildings, not easily accessible, were efficiently described thanks to the digital elevation model built based on a photogrammetric survey.

Preliminary measurement survey

The historical research brought to light the architectural plans (top view, cross and longitudinal sections) of the church dating back to different times. These plans were used as a starting point for the geometric survey. The actual thickness of the pillars and of some walls were assessed by simple ruler measure, while greater distances such as interpillar distances, height of the main nave vault and arches, of the lateral nave domes and arches, were acquired with a laser-based distance metre. As the extrados of the vault was accessible, it was also possible to determine the thickness of the vault through a pre-existing hole. This preliminary measurement survey was then completed by a close-range photogrammetry study.

Close-range Photogrammetry

Terrestrial and aerial close-range photogrammetry were performed to obtain a three-dimensional representation of the building's geometry.

Photogrammetry is the science of obtaining spatially distributed information from a set of images. As such, it is often employed to obtain three-dimensional measurements. Close-range photogrammetry is a subtype that collects information from shorter distances and different angles. Since the advent of digital cameras and more powerful computers, photogrammetry has become accessible as a tool outside of the photogrammetry profession. It is thus employed in many applications today, including structural engineering and cultural heritage [20,21]. In this project, image sets were obtained from ground and drone flights, further referred to as terrestrial and aerial photogrammetry, respectively.

Terrestrial photogrammetry was realised with a RICOH GR III fixed lens camera. Its CMOS sensor has a size of 23.5mm x 15.6mm and holds 24MPx. The lens's focal length is 18.3mm, which gives an approximate equivalent of a full-frame focal length of 28mm. Aerial photogrammetry was performed with a DJI Mavic Mini drone equipped with the DJI FC7203 camera. This camera has a 6.3mm x 4.7mm-sized CMOS sensor and holds 12MPx. The lens has a fixed focal length of 4.5 mm, which corresponds to a focal length of 24mm in the full-frame format equivalent. The aperture on this camera system is limited to f/2.8. Ground control points were obtained with a Leica Disto S910 in a relative coordinate system. The control points were later used to scale and orient the point cloud obtained through photogrammetry. Additional control points were acquired from the extrados of the vault to reconstruct its geometry.

The processing of the raw images was performed with the open-source software Raw Therapee. Image alignment, point-cloud, and mesh generation were performed with Agisoft Metashape Pro [22]. The 3D CAD tool Rhinoceros [23] was employed to extract cuts and sections from the three-dimensional mesh model. The same tool was further utilised to reconstruct a simplified model to analyse vault elements using three-dimensional analysis tools.

Structural Analysis

The structural analysis was executed by applying the Safe Theorem of Limit Analysis. With this theorem, a structure is considered safe if an admissible stress state in equilibrium with the applied loads is encountered. Heyman [9] provides an extension of limit analysis which can be applied to masonry structures given that three simplifying assumptions are adopted:

- masonry has null tensile strength;
- masonry has infinite compressive strength; and
- no sliding failure occurs.

These assumptions hold in most of the masonry buildings since the compressive stresses are low, usually two orders of magnitude below the compressive strength, and the structure is constructed carefully avoiding sliding failure.

Given these assumptions, an admissible stress state in masonry is equivalent to compressive force paths contained within the geometry of the structure. For 2D structures this compressive path is also known as the thrust line. A pseudo-3D analysis can be performed by slicing a three-dimensional geometry in a series of arches.

For the structural analysis of the St. Angelo Church the slicing technique [14] will be applied in the main nave vaults, checking for the local stability of these elements and

computing the adequate load transfer applied to the columns and buttresses. Later, the transversal section of the church will be analysed and a geometric safety factor is calculated showing how stable the structure is or, equivalently, how far it is from collapse. These simple analyses will be executed with the use of graphic statics and the construction of force polygons.
To validate the results and expand the analysis obtained with the slicing method, two three dimensional methods are applied: Membrane Equilibrium Analysis (MEA) [16,17] and Thrust Network Analysis (TNA) [18,19].

CASE STUDY: ST. ANGELO CHURCH

Location

St. Angelo church stands on St. Angelo hill, within the historic centre of Anagni located at the following coordinates 41°44’31”N 13°9’19”E. Figure 1 shows the Church and surrounding areas. The Church is part of a bigger complex comprising a convent and a rectory. The north side is adjacent to the convent while the south side faces the cliff. The Church lies on a wide substructure aimed at stabilising the ground pressure and at levelling the irregular local topography.



1. Back view of St. Angelo Church and surroundings

The plan, section, and the main façade (east) are depicted in Figure 2. The church is approximately 16.5 m wide and 20.9 m long. A 3.3 m long porch is seen before the main entrance door. The current building has a main nave approximately 5.50 m wide and two side aisles spanning 3.00 m. The longitudinal section of the Church can be divided into four main structural modules.

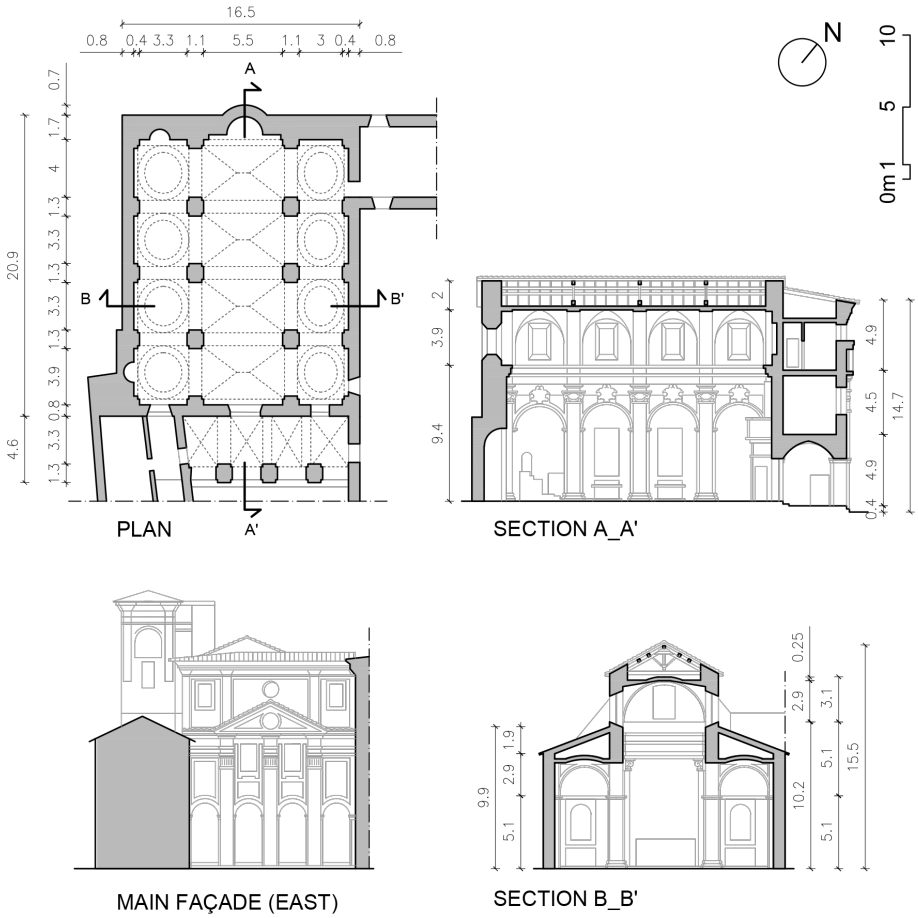

2. Plan, sections and east view of St. Angelo Church based on the survey

Construction phases

St. Angelo Church underwent several distinct construction phases during the past centuries; the historic analysis indicated 6 major phases (a-f), highlighted in the timeline of Figure 3 and described in this section. For each major phase, the corresponding changes in the west elevation view are highlighted in the detail of Figure 3.

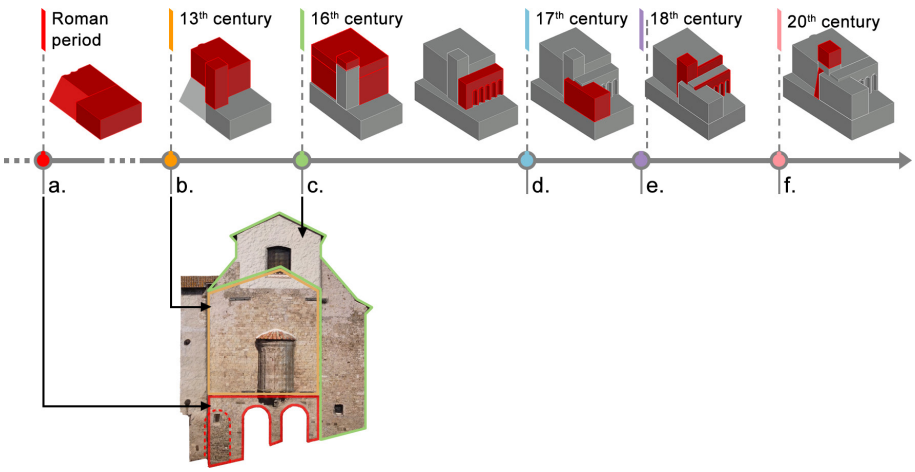

3. Constructive phases of St. Angelo church; on pictures below time-line, three phases were recognized with different colours basing on masonry texture

Each phase is described herein:

a. The substructure of the Church was built during Roman settlements in the area [24]. This substructure consists of a series of arches and vaults, and it was used as gathering space. Indeed, on the west side of St. Angelo church, an arch sequence is visible at the base of the building.
b. The first church was erected in the 13th century, in a Romanesque style. The dimensions and shape of the apse suggest the presence of a smaller church than the actual one, having one nave, timber trusses and a gabled façade. The apse was located on the west side of the structure, and it is still visible in the west façade (see orange line in Figure 3). During the same period, the left arch of the Roman substructure was filled to create a crypt (see dashed line in Figure 3), and a massive tower, with thick walls and vaults, was probably added.
c. A major transformation of the church happened around the 16th century, although the exact date is not documented [24]. The inner space was divided into a central nave and two aisles, which required the extension of the church southward and eastward, embedding the original tower within the structure, and, consequently, the enlargement of the plateau, whose slope was consolidated with ashlars. The nave was separated from the aisles by two rows of five pillars each. The nave was raised and a cross vault was built. In order to accommodate for the thrust of the vault, buttresses were added both on the north and south sides of the building. Figure 4a shows the north- and southward extensions highlighting the buttresses (green) added to carry the vaulting horizontal thrust, whereas Figure 4b depicts the north side where the added buttresses are embedded within the roof of the aisles and adjacent buildings.
d. On the eastern side, a 5-arches porch was added between the end of the 16th century and the beginning of the 17th century. The central arch was aligned with the longitudinal axis of the church, just as the first and last ones corresponded to the longitudinal axis of the aisles. The adjacent rectory was built during the 17th century by cutting the left part of the porch [24], which is still embedded in the rectory (Figure 4c).
e. During the 18th century, the appearance of St. Angelo church was adapted to the Neoclassical style. Stucco was extensively applied to renew the façade and to cover structural elements, thus changing their original shape. In the same period, the bell tower was reconstructed after an earthquake.
f. Finally, in the 20th century a new bell cell and a retaining wall were built to ensure stability of the main tower.



(a) (b) (c)

4. (a) South-west view of St. Angelo with highlights on the buttresses (green and pink). **(b)** North-east view of the building with highlights on the buttress. **(c)** East façade showing the porch

Restoration interventions

A series of interventions were applied on St. Angelo Church starting from the end of the 19th century [24], they can be divided into structural and non-structural interventions. Non-structural interventions included a new baptismal font and altar balustrade. A large window was added over the major altar. The roof was restored several times (in 1890, 1953, 1975, and 1994), as well as the floor (in 1935 and 1953). In 1958, the façade was restored and covered by marble slabs, which were then removed in 1992, thus bringing to light the original façade, made of stone units (Figure 5a). Figure 5b shows the juxtaposition and the dimension of the masonry units, highlighting the transformation processes of the church; in particular, one of the original arches of the 16th century porch can be seen in Figure 5c filled to and raised to match the elevation of the vaults in the porch.



5. Porch of St. Angelo church: **(a)** overview; **(b)** different dimensions in masonry units and metal tie rod, sutures are underlined in blue; **(c)** filling of a previous arch

Regarding structural strengthening actions, metal tie rods were inserted and the effectiveness of these actions will be discussed in the structural analysis. Along the longitudinal section (east-west), a pair of ties run below the floor and another run above the extrados of the main vault. Their anchors can be seen by looking at the exposed west façade in Figure 6. Along the transverse direction (north-south) two pairs were also installed, and are visible from the south façade (Figure 6).



6. Metal tie rods applied to St. Angelo church, south-west corner view: green is for older ties, blue is for more recent ones

Building materials

The knowledge of the structural elements of the case study in terms of materials and mutual connection is essential for a realistic structural analysis [25,26,27,28]. Figure 7 shows the various masonry types (0-3) recognized in St. Angelo Church during the field work. Four types were mainly identified based on the visible texture and correlated with the documented historical construction phases.

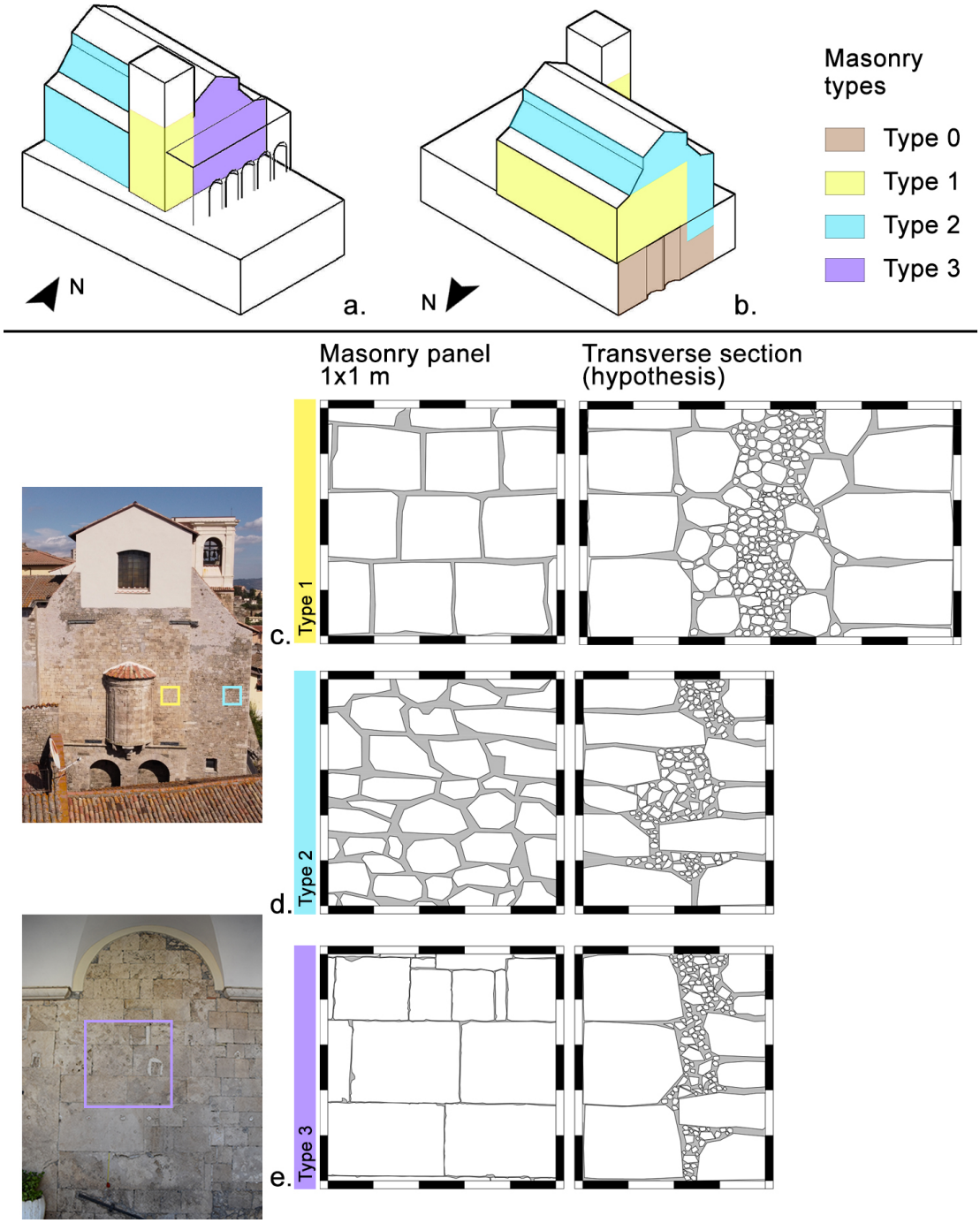

7. Above: identification of four masonry types on a 3D view of St. Angelo Church: **(a)** south-east and **(b)** north-west corners. Below (from **(c)** to **(e)**): masonry textures and hypothesis of transverse sections

The types of masonry are briefly described herein:

- Type 0: The substructure consists of well-arranged stone ashlars and thin mortar joints, with considerable thickness
- Type 1: In the 13th century church, coursed stone ashlars with various sizes laying on thin mortar joints are observed. The specific weight (ρ) of type 1 was assumed equal to 22 kN/m^3, according to [29]. The transverse section of the church walls is probably made of three leaves, i.e., the outer ones of travertine ashlars and the inner core of stone fragments, pebbles and mortar (see Figure 7c).
- Type 2: Renaissance additions were built with a lower quality: mortar joints are wider compared to those of the original construction and stone units are unhewn (Figure 7d). The scarce arrangement of the masonry led to the hypothesis that the transverse section of the wall was made of three leaves, the outer ones with fieldstone, the internal core of rubble stone. More attention was paid to the edges of the wall, in which quoins were adopted to regularise the corner. A specific weight of 20 kN/m^3 was assumed according to regulations from the Ministry of Infrastructures and Transportations [30].
- Type 3: The last type observed corresponds to the newest additions in the church, present in the east façade. As this façade corresponds to the entrance, the masonry quality is apparently better. The outer leaf has well-cut travertine ashlars laying on very thin mortar joints. Similarly to the west façade, one may suppose that the other leaf (toward the interior of the church), which is plastered, should have been made of scarcely arranged fieldstone. An incoherent inner core might have been interposed between the outer leaves (Figure 7e). The same specific weight of 20 kN/m^3 was assumed adopted for this type [30].

It is maybe worth mentioning that masonry typologies could only be analysed and classified according to their *external* appearance. The presence of transversal connections, could have been checked by inspecting the internal structure of the wall via, as an example, endoscopic inspections.

Columns within the church are plastered (Figure 8a); nonetheless, similarly to the cathedral of Anagni, they are presumably made of travertine units and voussoirs. Regarding horizontal structures, the intrados of the main nave structural vault is plastered (Figure 8a), whereas the extrados is covered by mortar (Figure 8b). The irregular surface of the vault's extrados led to the hypothesis of a vault made of fieldstone and lime mortar, with a specific weight of 20 kN/m^3. A thickness of 0.25 metres was measured. The extrados of the vault is partially backfilled by loose material, e.g., earth and stone fragments (Figure 8c), whose specific weight was supposed to be 14 kN/m^3 [31] and whose presence is recognized to be beneficial to the load distribution inside the vault. The height of the filling is 1.20 metres. The roofing system is composed of timber trusses resting on sockets in bearing walls, which sustain double-framed timber joists and wooden plank. The wood species could not be identified; therefore, a specific weight of 4.50 kN/m^3 (spruce) was assumed according to [32].

Figure 9 summarises materials and weights of structural elements composing the bearing system of the church.



8. (a) Cross vaults in the interior of St. Angelo. **(b)** Timber roof structure above the vaults and **(c)** filling of the vaults and detail of the roof support showing also the texture of bearing walls (fieldstone)

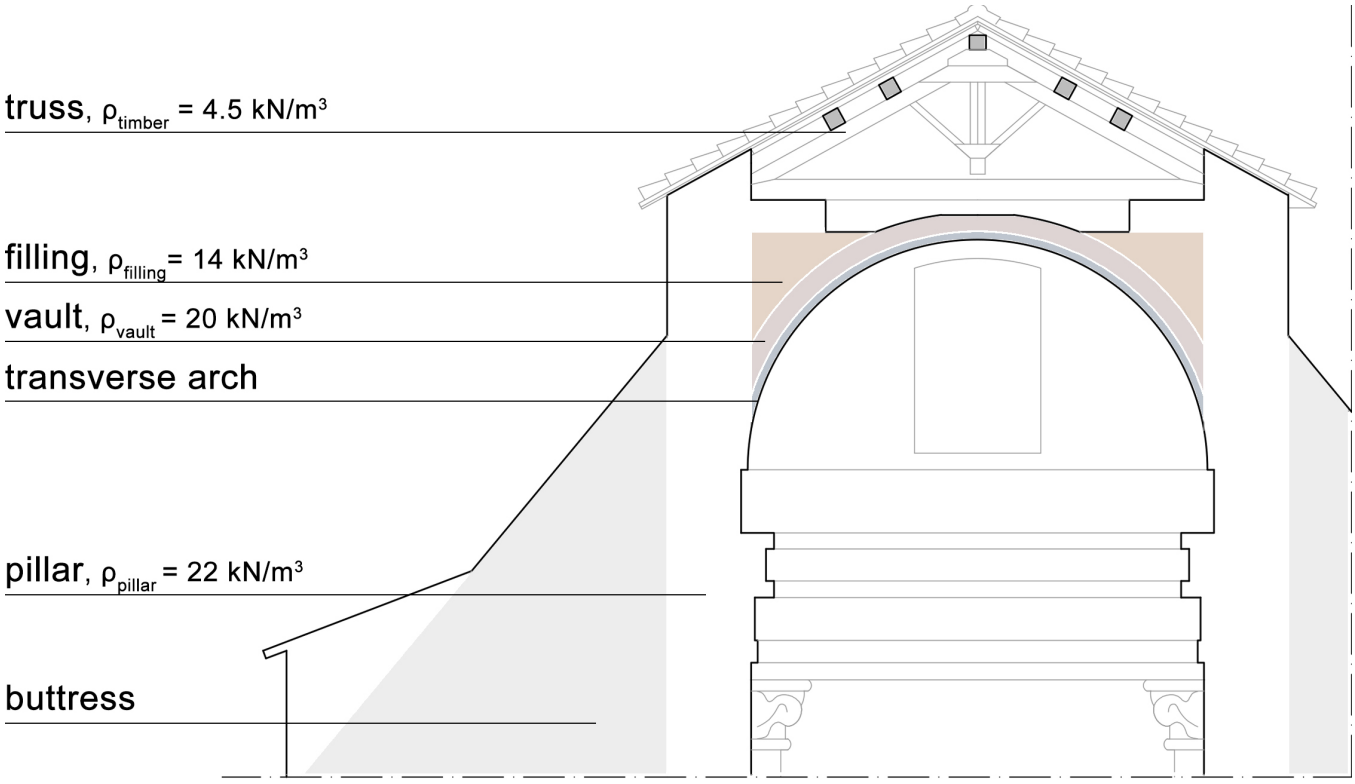

9. Longitudinal typical section showing the specific weight assumed for materials.

GEOMETRY RECONSTRUCTION

Photogrammetry expedition

The photo capture on the inside of the building was executed taking approximately 300 images. Low light conditions inside the Church were a challenge to this process as the quality of the images is directly associated with the lighting condition. The aperture on the camera was fixed to f/5.6 to generate a depth of field to capture architectural elements positioned at different distances to the lens while providing enough light sensitivity for the low light conditions. Shooting time was set to 1/30s, generally low, but produced acceptable results as the camera is equipped with a three-axis sensor-shift image-stabilisation system. The ISO-setting was left to automatically adapt to the lighting situation, allowing production of images with lower ISO (lesser noise) when the lighting was more robust, and still capturing images in the least favourable lighting situations with high ISO (more noise).

Given the geographic conditions around the building only the Church entrance (east façade) could be captured by terrestrial photogrammetry, and thus a drone mission was flown to complete the imaging survey. The drone mission also allowed capturing images of the roofing and the broader topographical context of the structure. On this drone model, the aperture was restricted to f/2.8; the resulting limited depth of field was not a major issue, as the camera's distance to the object was usually more than 10m. The daylight situation allowed for a fixed ISO-setting of 100. The exposure was defined by shutter priority, shooting faster than 1/600s. 110 images were captured. Considering the densely constructed area surrounding the church, it is worth noting that the potential loss of signal and the restricted battery life posed important challenges. Two overflights were required to complete the imaging campaign.

To scale the photogrammetry output, four ground control points (GCPs) were defined inside of the church. Two were placed on the sites of the nave at the entrance, another across the central nave close to the altar, and the last one towards the centre of the limit of the north lateral nave. Outside GCPs were defined on easily identifiable features mainly on the eastern façade, and captured by both the drone and the terrestrial photo capture.

Point Cloud Generation

For the image alignment process, the downscaling factor of the images was set to 4, corresponding to Metashape's «Medium» accuracy setting. The photos taken in the low light setting were of suboptimal quality, and thus the average pixel obtained through downscaling was more meaningful and computationally efficient.

The resulting sparse cloud describes matched image points and estimated camera positions. The cloud was then cleaned, meaning that points of no significance or those not representing the real context were eliminated. Finally, a realignment of the points was executed. In the next step a dense cloud was generated extracting the depth information of each image. For this purpose the images were downscaled by a factor of 8 which corresponds to Metashape's «Medium» quality setting.

An aggressive depth filter algorithm was applied to treat the high noise in the images caused by the elevated ISO-values of the camera settings in accounting for the sub-optimal lighting conditions.

The images from the exterior were processed in two separate chunks for the terrestrial and the aerial image set, reciprocally. They were then aligned based on characteristics in the dense-point cloud within Metashape.

Model Postprocessing

Based on the dense-point cloud, a textured mesh model was calculated with approximately 450.000 faces in the exterior mesh and 2.600.000 faces in the interior face. The difference in the number of faces and precision of the meshes is directly related with the scene complexity and detail representation in the image sets. In addition, the drone's wide-angle lens resulted in multiple adjacent buildings being captured and only later excluded in the postprocessing. A texture was built for the surface and finally the mesh model was exported as a *.obj* file to be further treated with Rhino 3D. To align interior and exterior meshes the highly recognizable traces of the façade, such as the arcade and plaster details served as natural feature connection among the internal and external image capture. Additionally, knowing the thickness of eastern and southern wall the alignment of the meshes could be checked.

The Internal and External meshes are depicted in Figure 10.



10. Final Model: **(a)** External mesh composed of approximately 450.000 faces **(b)** Internal mesh composed of approximately 2.600.000 faces

STRUCTURAL ANALYSIS

The main elements of the Church were identified and a structural analysis was conducted in order to assess the stability of the main structural elements of the church. We report here the analysis executed for the vault in the central nave as a single element, as well as the for the main transversal section evaluating the geometric safety factor. The main measures of the plan and the typical cross section of the Church are depicted in Figure 2. Figure 11 zooms in one module the Church that has been considered in the structural analysis, with more detailed measurements.

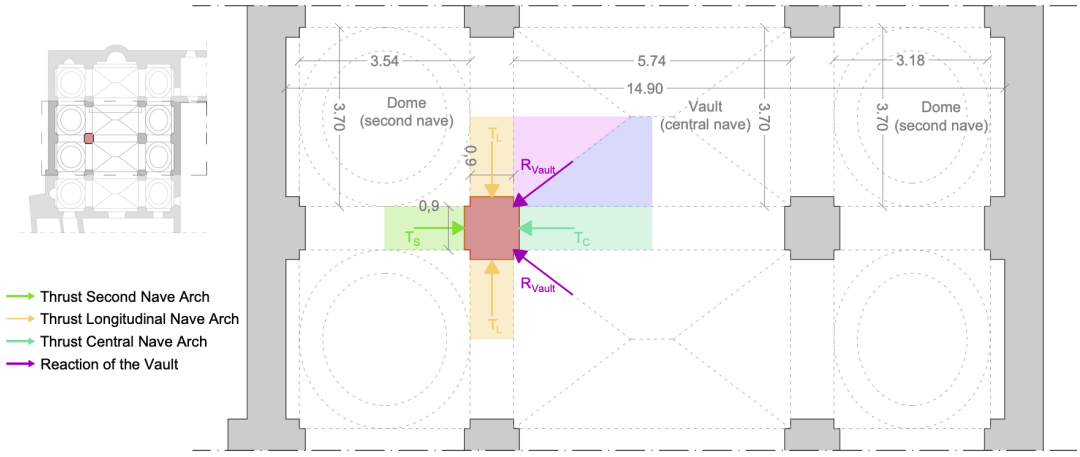

11. Main dimensions of the typical transverse module of the church, and highlight the column used to check the GSF

Stability of the main vault

The stability of the vault has been assessed with a graphic static method using a slicing technique [14,33]. The typology of the rectangular vault analysed is a mix between a barrel vault with lunettes and a cross vault, justifying the application of the slicing technique. Adopting this approach, the vault is sliced and each individual section is considered separately. The thrust line should be contained within the intrados and extrados of each slice and converge to the diagonal, where a fictitious arch should also constraint the resulting diagonal thrust line. Only the corners of the vault are considered to thrust on the buttresses, meaning that no thrust is transmitted directly to the walls of the church. For the present analysis the infill is considered as a weight but the thrust line is now allowed to travel through it, which is a conservative assumption.

Two directions (x and y), and four slices per each direction with a spacing of 0.60 m (b_x) and 0.42 m (b_y) were considered respectively, over the total dimensions of the vault, 5.74 m (L_x) per 3.34 m (L_y), as represented in Figure 12. Each slice identifies an arch labelled as A, B, C and D going from the boundaries to the key of the vault. The geometry of the slices, i.e. the intrados and extrados elevation is extracted directly from the digital model depicted in Figure 10.

The thrust lines of each sliced arch have to be contained within the intrados and the extrados of the slices and fulfil two additional following constraints. The first one is given by the horizontal components of the thrusts (i.e., H_{Ax} and H_{Ay}). Indeed, they should be in such a ratio that their sum (i.e., H_A) is tangent to the diagonal of the vault. A second constraint is imposed by the elevation of the end point in each slice, as they should coincide for the two directions. Once these constraints are satisfied, a thrust line is found within the thickness of each sliced arch, and the point of application of the thrusts in the diagonal is defined. The magnitude and inclination of the forces acting in the diagonal is also computed by summing the vectors at perpendicular slices yielding (i.e., $R_A = R_{Ax} + R_{Ay}$). With the position and magnitude of the resultants from the slices, the force polygon of the diagonal arch is drawn assuming a given horizontal thrust at the key (H_{key}) and ensuring that the diagonal thrust line lies among intrados and extrados. From the diagonal force polygon, the magnitude of the horizontal thrust at the rib of the diagonal arch, H_{vault}, can be computed as 24.6 kN, while the vertical component, W_{vault} (or the weight of one quarter of the vault) is equal to -34.8 kN, corresponding to an inclination H/W = 70.7%.

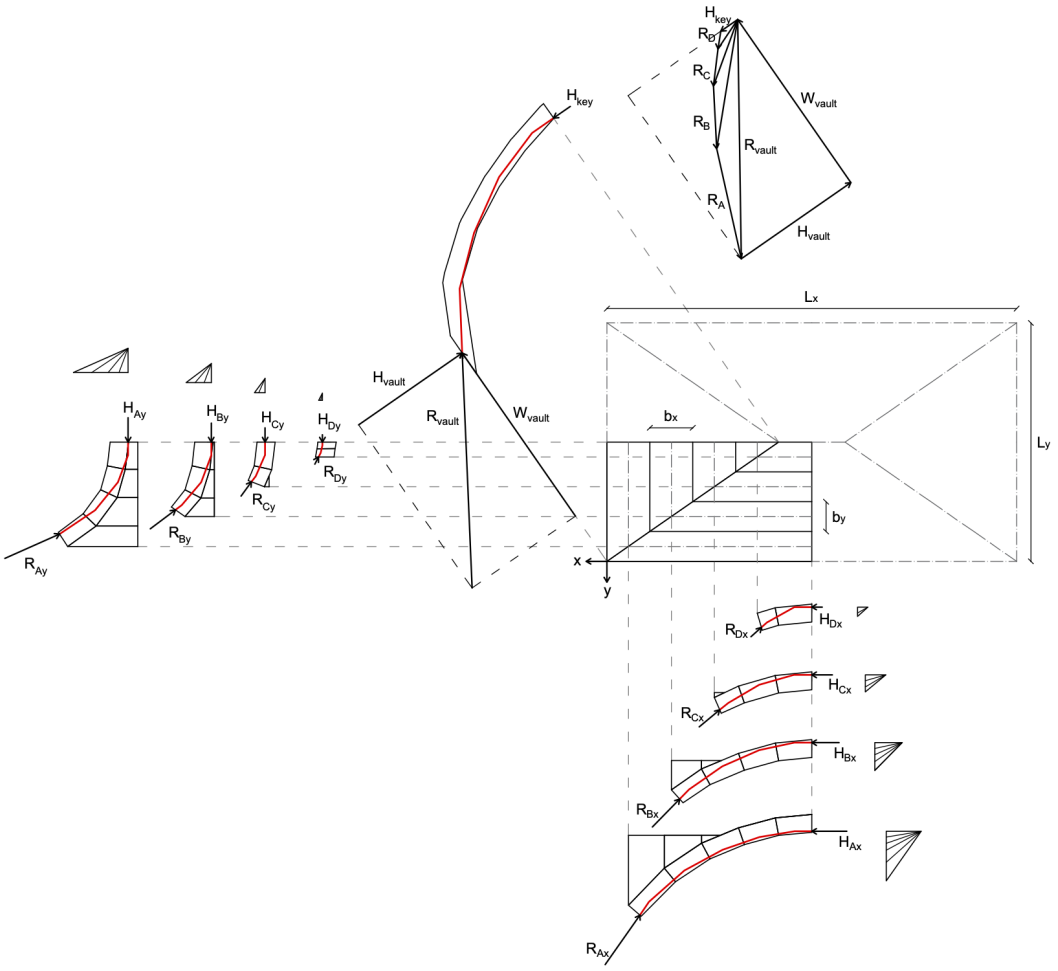

12. Thrust lines of sliced arches and fictitious diagonal arch: drawing of the force diagram for the estimation of the horizontal and vertical thrust at the rib of the diagonal arch to be transmitted to the buttressing system

Global section analysis

The calculation outlined in the previous paragraph served the purpose of obtaining the thrust of the cross vault, concurring with the other forces to the global equilibrium of the column highlighted in Figure 11. The calculation of the geometric safety factor for this element should be considered as an example but given the symmetry and the geometric configuration of the problem, the Authors have assumed it to be a sufficiently *general* case to refer to. Same calculations should be performed on the other columns and on the walls to assess the global stability and derive a safety factor for the entire structure. The sectional analysis was conducted considering the forces of the structural elements that converge into the column highlighted in Figure 11, that is the vault's reaction (R_{vault}), the thrust of the arch in the central nave (T_C), the arch of the second nave (T_S) and the weight of the walls on the top of the pillar (W_{UV}).

Conservatively, the horizontal thrusts of the longitudinal arches between the two naves and of the domes of the lateral nave were not considered in the global equilibrium. Indeed, the horizontal forces coming from the longitudinal arches (T_L), represented in Figure 11, will cancel each other, thus, the only non-zero contribution is the vertical component, with a stabilising effect. As for the domes, the horizontal components will be opposite to the thrust coming from the vault and the vertical components will act as well as stabilising.

To better compute the volume of the elements and then their weight, following the assumptions described on Figure 9, the typical cross section of the church is divided into four different blocks, coloured in blue, green, red (for the main nave pillar) and yellow (for the external nave pillar). The force and moment equilibrium of each of these blocks is assessed separately at the bottom of the block. Figure 13 represents a transversal and a longitudinal section of the church with such partitioning. The forces applied in each block are named and numbered at Table 1 and the resultant thrust line in the transversal section is depicted in Figure 14.



13. Longitudinal (B-B') and Transversal (A-A') sections of the church with highlights on the four blocks considered in this global analysis.

Analysing the first portion (highlighted in blue), the acting loads include self-weight W_{uw}, accounting for the tributary volume in the longitudinal direction, and the weight of the roof W_{roof}. Two inclined forces also act on the block: the thrust of the vault T_{vault} (calculated in the previous paragraph) and the thrust of the arch T_{arch} of the main nave. The equilibrium in this block is verified considering the resultant $R_{2/1}$ acting with an eccentricity $x_{2/1}$ measured with respect to the column axis (Table 1). This resultant will then be transmitted to the following block.

In the central portion of the column (highlighted in green), the force carried from the first part is applied $-R_{2/1}$ and added to its self-weight W_{iw}, as well as the thrust coming from the lateral arch $T_{lateral\text{-}arch}$ and the thrust of the buttress $T_{buttress}$. We consider a thickness of 40 cm to the buttress, following the geometric survey. In these calculations, $T_{buttress}$ is the unknown of the problem and is determined by such that it maximises the geometric safety factor at the base of the pillars subjected to still containing a thrust line inside the geometry of the buttress. The value after optimisation is presented in Table 1 marked with an asterisk (*). Finally, the equilibrium of the forces acting in the second block results in the reaction transmitted $R_{3/2}$ acting with eccentricity $x_{3/2}$.

The bottom of the column (highlighted in red) only bears its self-weight W_{pillar} and the action coming from the block above $-R_{3/2}$, and transmits these loads to the ground, resulting in a base reaction $R_{0/3}$ applied with an eccentricity $x_{0/3.}$

The corresponding load paths, from the upper parts of the church to the ground, is represented in Figure 14. Table 1 summarises the magnitude of the different forces pertaining to the "thrusting structural elements" such as Vault, Arch, Buttress, both vertical and horizontal components along with their eccentricity with respect to the pillar/wall axis. The combination of vertical and horizontal force components lied within the wall/pillar width, thus entailing the global stability of the structure.

Focusing on the lateral wall, similar calculations lead to the force distributions reported in Figure 14 and Table 1.

Nomenclature	Component		Eccentricy from the axis of the pillar	Elevation from the ground
	Vertical (z)	Horizontal (x)		
Upper block - main nave pillar				
W_{roof}	-15	0	0.15	N.A.
W_{uw}	-198	0	0	N.A.
T_{vault}	-70	-40	0.45	10.3
T_{arch}	-41	-16	0.45	10.3
$R_{2/1}$	***323***	***56***	***$x_{2/1}$=0.16***	***10.3***
Middle block - main nave pillar				
$-R_{1/2}$	-323	-56	0.16	10.3
W_{iw}	-350	0	0	N.A.
$T_{buttress}$	-45	**30***	-0.45	9.7
$T_{lateral\ arch}$	-20	8	-0.45	5.05
$R_{3/2}$	***761***	***18***	***$x_{3/2}$=-0.17***	***5.05***
Lower block - main nave pillar				
$-R_{2/3}$	-761	-18	-0.17	5.05
W_{pillar}	-138	0	0	N.A.
$R_{0/3}$	***900***	***18***	***$x_{0/3}$=-0.24***	***0***
Lateral nave wall				
W_{roof}	-11	0	0.15	N.A.
$T_{buttress}$	-47	**30***	0.6	7
$T_{lateral\ arch}$	-20	-8	0.6	5.2
W_{iw}	-632	0	0	0
$R_{0/4}$	***652***	***19***	***$x_{0/4}$=-0.32***	***0***

Table 1. Forces acting in the transverse cross section of the church. Forces indicated in kN with positive upwards and towards the right. Distances indicated in m.

From these analysis, it is possible to define a geometrical coefficient of safety (GSF) as, for example, introduced by Huerta [34]:

$$GSF = \frac{h/2}{e} \tag{1}$$

where h is the thickness of the pillar and e is the eccentricity of the resultant applied in the pillar. It is of interest to determine the GSF with respect to the base of both pillars using the eccentricities $x_{4/0}$ and $x_{3/0}$ calculated in Table 1 after an optimisation against the thrust of the buttress executed with a trial-and-error method.

The results obtained show a GSF of 1.9 for the base of the main pillar, whose structural radius is assumed to be 90 cm, and 1.9 for the base of the lateral nave pillar, whose structural radius is assumed to be 1.2 m. Geometrically, this corresponds to a thrust path staying near the middle half of the pillars, as depicted in Figure 14.

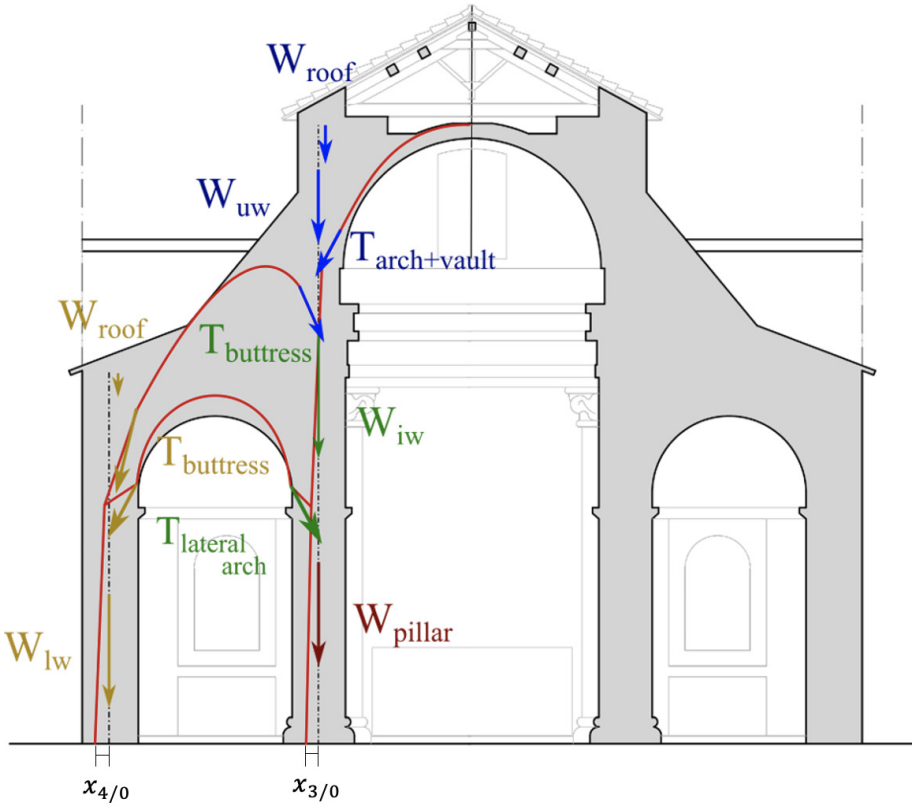

14. Thrust line obtained in the global transversal section of St. Angelo Church showing the forces applied to the blocks and the eccentricity obtained in the base of the pillars $x_{0/3}$ and $x_{0/4}$.

It must be acknowledged that geometric safety factors are usually around 3 or 4; however, as the determination of the GSF relies on the static approach of limit analysis, this value is an underestimation of the real GSF of the church, which can then be reasonably considered safe with respect to the loads considered and the safe assumptions taken, such as not considering the dome between the columns in the side aisle.

This study also underlines the important stabilising effect of the buttress. In fact, not considering this force would result in a higher eccentricity $x_{0/3}$ and, therefore, in a drop of the safety factor to 0.8 for the main nave pillar. As for the pair of ties observed in Figure 6, the present analysis concluded that the church is safe under gravity loads and therefore these ties are not needed. However, the action of seismic loads was beyond the scope of this paper and were not analysed. Given the seismic activity of Anagni region, the Authors suppose that the ties were added to account for such seismic loads, however further investigation would be needed to determine its effectiveness.

Finally, the compressive force at the bottom of the pillar is around 1 MPa, which is much lower than the compressive resistance of the ashlar composing the pillars, thus excluding a failure of this element in compression.

Thrust Network Analysis

In this section, the cross vault in the main nave is revisited with Thrust Network Analysis (TNA) to validate and expand the results obtained. TNA is a direct extension of the discrete application of the lower-bound theory to three-dimensions. In TNA, instead of finding one thrust line that is found in the envelope of a 2D structure we impose that a force network carrying compressive axial force in the edges is contained within the three-dimensional intrados and extrados of the vault. The method was developed by [18] and applied to vaulted masonry structures in [19] in combination with optimisation algorithms with different objective functions. To the analysis with TNA, the input required is the form diagram containing information about the topology of the internal force flow and the boundary conditions.

Figure 15a shows the input used for the analysis: the form diagram is chosen following the same rationale as the slicing technique. This network will be constrained to fit between the intrados and extrados of the vault such that each node *i* has its elevation constrained between the elevations of the intrados (z_i^{LB}) and extrados (z_i^{UB}). The filling observed in the vault is added as self-weight to the corresponding nodes, not acting as structural element, which is a conservative approach. With such inputs, a constrained nonlinear optimisation is formulated and solved to find the thrust network minimising the horizontal thrust of the problem. The thrust network obtained is presented in Figure 15b with highlight to the resulting reaction force R_{vault} = 47.9 kN, and inclination H/W = 60.6%, which is smaller than the one found with the slicing method. If this thrust inclination is transferred to the global analysis, the horizontal component of the vault's thrust is reduced by a factor of 6/7 and the GSF increases to 2.1, reducing the conservatism of the analysis. With the use of such a method additional analysis can be performed such as finding maximum load multipliers to hazardous external loads, however we limit the scope of the paper to the analysis to gravity loads.

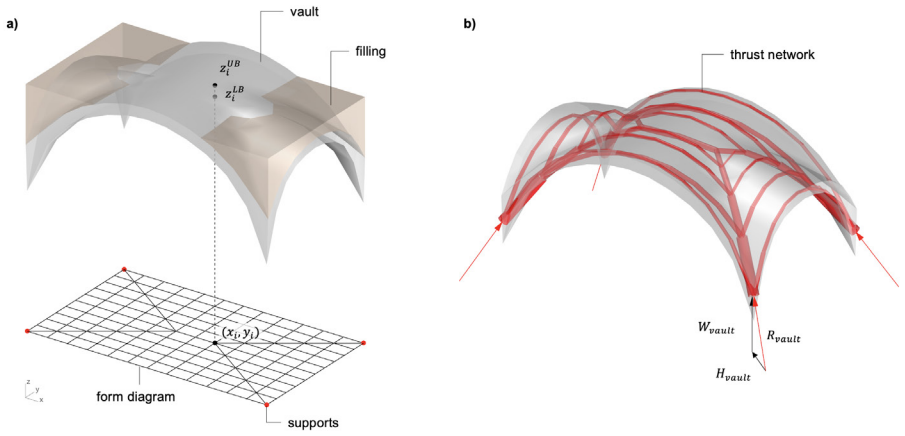

15. (a) Input required for the TNA analysis: form diagram, with the topology of the internal forces; geometry of the vault extracted from the survey constraining the elevation of the nodes between z_i^{LB}, z_i^{UB} and filling applied as a load to the corresponding nodes. (b) Result of the analysis showing a Thrust Network inside the geometry of the vault with highlights to the reaction vector R_{vault} and its decomposition.

Membrane Equilibrium Analysis

This section revises the equilibrium of the main vault by applying a 3D membrane analysis. According to the Safe Theorem of Limit Analysis, if it is possible to find a purely compressed thrust surface (membrane) of a certain thickness, in equilibrium with the applied loads, contained entirely within the thickness of the vault, then the structure is stable. In this section, the Membrane Equilibrium Analysis (MEA), introduced in [16] and applied for the equilibrium of complex vaulted structures in [17], is here applied to the cross vault of the St. Angelo Church.

Given the load (self-weight and vault filling) as described in the previous sections, there are two ways to achieve the results. The first one is choosing the shape and finding the stress function (Airy stress function) under which that shape is purely compressed (a convex Airy stress surface), and the second one is to find the equilibrated membrane given an assigned stress function. Henceforth, the first approach is used, and the proposed shape for the membrane is one among the possible solutions of the equilibrium equations (see Figure 16).

The desired surface was searched by modifying some shape parameters with the constraint that this was compressed under the assigned loads.

Supposing the membrane thickness of 4 cm, the analysis results give the principal stress along the surface as shown in Figure 17 and a thrust along the diagonal arches equal to 38 kN. The main advantage of using this method is that the stresses directions and distribution are straightforward upon the membrane (as shown in Figure 17) at every point. The values of the stresses reported are considerably smaller compared to the compressive strength of the masonry.

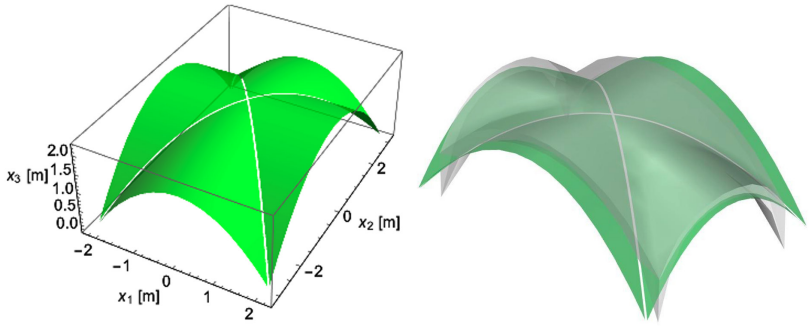

16. Left, Compressed membrane. Right, Membrane surface within the cross-vault intrados and extrados.

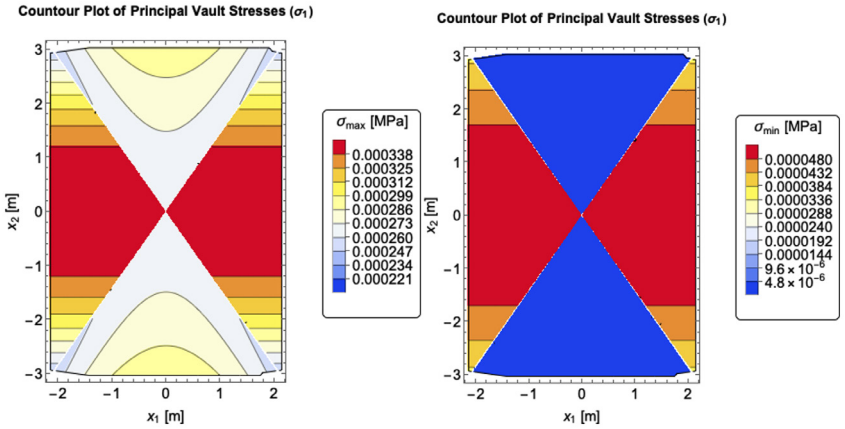

17. Colour plot showing the magnitude of the principal stresses in the membrane. Left: stresses in the principal direction σ_1 Right: stresses in the principal direction σ_2

CONCLUSIONS

Through a combination of coherent and appropriate use of modern technologies for geometrical survey and simple and clear mechanical theories, this paper shows how in pressing time and with simple means, a multidisciplinary group including architects, conservators, and structural engineers carried out a preliminary structural assessment of St. Angelo Church under gravitational loads.

The results obtained and reported in this paper show the pipeline adopted during the course, emphasising how it can be applied to historic structures and can serve the interest of practitioners in the field of structural preservation and researchers interested in modern applications of limit analysis theory.

A key ingredient of the procedure described is a faithful description of the geometry and the identification of loads and their distribution. The experience held in Anagni, whose methodological aspects and main outcomes have been summarised in this paper, has shown the powerful analysis tools that can be implemented referring to limit analysis principle, combined with digital survey tools. The powerful static equilibrium approach in Heyman's theory and related calculation tools have the fundamental advantage of not relying on any material characterization, provided the masonry is recognized as complying with the fundamental hypothesis of infinite compressive strength. As such, this whole methodology specifically suits historic masonry buildings, for which performing in situ mechanical characterization or taking samples could be extremely difficult or even impossible due to the need to limit invasiveness. The results show that the Church is safe under gravitational loads with sufficient safety factors. Additional analysis concerning the effects of usual design lateral loads (wind or earthquake) is beyond scope of the present paper. Nonetheless, what was proposed could effectively represent a methodology to preliminary assess the vulnerability of existing structures, targeting more accurate and sophisticated numerical modelling which would naturally benefit from the geometrical reconstruction. Moreover, if leaning vertical elements, cracks, differential settlements profiles are recognised at this stage, the more computationally demanding analyses may be focused on these portions rather than on the entire structure, saving significant amount of time and computing resources, leaving some space to the adoption of more sophisticated constitutive assumptions.

REFERENCES

[1] Ciocci, M.P., Sharma, S. and Lourenço, P.B., 2018. "Engineering simulations of a super-complex cultural heritage building: Ica Cathedral in Peru". Meccanica, 53(7), pp.1931-1958.

[2] ICOMOS/ISCARSAH Committee. 2003. Recommendations for the analysis, conservation and structural restoration of architectural heritage. ICOMOS 14th General Assembly, Vicoria Falls, Zimbabwe, October.

[3] Lubowiecka, I., Arias, P., Riveiro, B. and Solla, M., 2011. "Multidisciplinary approach to the assessment of historic structures based on the case of a masonry bridge in Galicia (Spain)". Computers & structures, 89(17-18), pp.1615-1627.

[4] Arias, P., Herraez, J., Lorenzo, H. and Ordonez, C., 2005. "Control of structural problems in cultural heritage monuments using close-range photogrammetry and computer methods". Computers & structures, 83(21-22), pp.1754-1766.

[5] Roca, P., Cervera, M., Gariup, G. and Pela, L., 2010. "Structural analysis of masonry historical constructions. Classical and advanced approaches". Archives of computational methods in engineering, 17(3), pp.299-325.

[6] Como, M., 2013. "Statics of historic masonry constructions (Vol. 1)", Springer, Berlin.

[7] Huerta, S., 2006. "Galileo was wrong: the geometrical design of masonry arches". Nexus Network Journal, 8(2), pp.25-52.

[8] Iannuzzo, A., Dell'Endice, A., Van Mele, T. and Block, P., 2021. "Numerical limit analysis-based modelling of masonry structures subjected to large displacements". Computers & Structures, 242, p.106372.

[9] Heyman, J., 1966. "The stone skeleton". International Journal of solids and structures, 2(2), pp.249-279.

[10] Heyman, J., 1982. "The Masonry Arch". Longman Higher Education.

[11] Hooke, R., 1974. "A description of helioscopes and some other instruments" (No. 3). TR.

[12] Poleni, G., 1848. "Memorie istoriche della gran cupola del tempio vaticano, e de'danni di essa, e de'ristoramenti loro, divise in libri cinque ..." Padova: Stamperia del Seminario.

[13] Wolfe, W.S., 1921. "Graphical analysis: a text book on graphic statics". McGraw-Hill book Company, Incorporated.

[14] Huerta Fernández, S., 2004. "Arcos, bóvedas y cúpulas. Geometría y equilibrio en el cálculo tradicional de estructuras de fábricaArcos, bóvedas y cúpulas. Geometría y equilibrio en el cálculo tradicional de estructuras de fábrica". Instituto Juan de Herrera, Madrid.

[15] Cennamo, C., Cusano, C. and Angelillo, M., 2019. "A limit analysis approach for masonry domes: the basilica of San Francesco di Paola in Naples". International Journal of Masonry Research and Innovation, 4(3), pp.227-242.

[16] Fraternali, F., Angelillo, M. and Fortunato, A., 2002. "A lumped stress method for plane elastic problems and the discrete-continuum approximation". International journal of solids and structures, 39(25), pp.6211-6240.

[17] Olivieri, C., Fortunato, A. and DeJong, M., 2021. "A new membrane equilibrium solution for masonry railway bridges: the case study of Marsh Lane Bridge". International Journal of Masonry Research and Innovation, 6(4), pp.446-471.

[18] Block, P. and Ochsendorf, J., 2007. "Thrust network analysis: a new methodology for three-dimensional equilibrium". Journal of the International Association for shell and spatial structures, 48(3), pp.167-173.

[19] Maia Avelino, R., Iannuzzo, A., Van Mele, T. and Block, P., 2021. "Assessing the safety of vaulted masonry structures using thrust network analysis". Computers and Structures, 257, p. 106647.

[20] Bedford, J., 2017. Photogrammetric Applications for Cultural Heritage: Guidance for Good Practice (J. Bedford, Ed.). Historic England.

[21] Stylianidis, E., 2020. Photogrammetric Survey for the Recording and Documentation of Historic Buildings. Springer International Publishing.

[22] AgiSoft PhotoScan Professional - Version 1.8. 2021. Retrieved from http://www.agisoft.com/

[23] McNeel R., Rhinoceros. 2021. Rhino - Rhinoceros 3D: http://www.rhino3d.com.

[24] Formosa F., Macetelli M., Di Cioccio A., 1994. "La chiesa di S. Angelo", Comune di Anagni, Istituto di storia e di arte del Lazio meridionale, Soprintendenza per i beni ambientali e architettonici del Lazio, Anagni. (in Italian)

[25] Giuffrè, A., 1993. Sicurezza e conservazione dei centri storici. Il caso Ortigia, 279. (in Italian)

[26] Anzani, A., Cardani, G., Condoleo, P., Garavaglia, E., Saisi, A., Tedeschi, C., Tiraboschi, C. and Valluzzi, M.R., 2018. "Understanding of historical masonry for conservation approaches: the contribution of Prof. Luigia Binda to research advancement". Materials and Structures, 51(6), pp.1-27.

[27] Betti, M., Bonora, V., Galano, L., Pellis, E., Tucci, G. and Vignoli, A., 2021. "An Integrated Geometric and Material Survey for the Conservation of Heritage Masonry Structures". Heritage, 4(2), pp.585-611.

[28] Borri, A., De Maria, A., 2019. Qualità muraria secondo il metodo IQM: aggiornamento alla Circolare esplicativa n.7 del 2019, Structural 222, Marzo-Aprile 2019, Paper 07.

[29] Leoni, G., Gara, F. and Morici, M., 2021, August. Evaluation of Seismic Vulnerability of the Historical SS Filippo e Giacomo Masonry Arch Bridge in Ascoli Piceno (Italy). In International Conference of the European Association on Quality Control of Bridges and Structures (pp. 613-622). Springer, Cham.

[30] MIT 2019, Ministry of Infrastructures and Transportations, Regulation no. 7/2019, Istruzioni per l'applicazione dell'«Aggiornamento delle "Norme tecniche per le costruzioni"» di cui al decreto ministeriale 17 gennaio 2018. (in Italian)

[31] Gelfi, P. and Capretti, A., 2001. "Backfill role on the stability of arches and vaults". WIT Transactions on The Built Environment, 55.

[32] UNI 11035-2:2010, "Legno strutturale - Classificazione a vista dei legnami secondo la resistenza meccanica - Parte 2: Regole per la classificazione a vista secondo la resistenza meccanica e valori caratteristici per tipi di legname strutturale". (in Italian)

[33] O'Dwyer, D., 1999. "Funicular analysis of masonry vaults". Computers & Structures, 73(1-5), pp.187-197.

[34] Huerta, S., 2010. "The safety of masonry buttresses". Proceedings of the Institution of Civil Engineers-Engineering History and Heritage, 163(1), pp.3-24.